Swift Discovery of Gamma-ray Bursts without Jet Break Feature in their X-ray Afterglows

G. Sato[1,2], R. Yamazaki[3], K. Ioka[4], T. Sakamoto[1,5], T. Takahashi[2,6], K. Nakazawa[2],
T. Nakamura[4], K. Toma[4], D. Hullinger[1,7,8], M. Tashiro[9], A. M. Parsons[1], H. A. Krimm[1,10],
S. D. Barthelmy[1], N. Gehrels[1], D. N. Burrows[11], P. T. O'Brien[12], J. P. Osborne[12],
G. Chincarini[13,14], and D. Q. Lamb[15]

ABSTRACT

We analyze *Swift* gamma-ray bursts (GRBs) and X-ray afterglows for three GRBs with spectroscopic redshift determinations — GRB 050401, XRF 050416a, and GRB 050525a. We find that the relation between spectral peak energy and isotropic energy of prompt emissions (the Amati relation) is consistent with that for the bursts observed in pre-*Swift* era. However, we find that the X-ray afterglow

[1]NASA Goddard Space Flight Center, Greenbelt, MD 20771, USA

[2]Institute of Space and Astronautical Science JAXA, Kanagawa 229-8510, Japan

[3]Department of Physics, Hiroshima University, Higashi-Hiroshima 739-8526, Japan

[4]Department of Physics, Kyoto University, Kyoto 606-8502, Japan

[5]Oak Ridge Associated Universities, P. O. Box 117, Oak Ridge, TN 37831, USA

[6]Department of Physics, University of Tokyo, Bunkyo, Tokyo 113-0033, Japan

[7]Department of Physics, Brigham Young University, Rexburg, ID 83440, USA

[8]Department of Physics, University of Maryland, College Park, MD 20742, USA

[9]Department of Physics, Saitama University, Saitama 338-8570, Japan

[10]Universities Space Research Association, Columbia, MD 20744, USA

[11]Department of Physics, Pennsylvania State University, University Park, PA 16802, USA

[12]Department of Physics and Astronomy, University of Leicester, Leicester, LE 1 7RH, UK

[13]Università degli studi di Milano-Bicocca, Dipartimento di Fisica, Italy

[14]INAF-Osservatorio Astronomico di Brera, Via E. Bianchi 46, 23807 Merate(LC), Italy

[15]Department of Astronomy and Astrophysics, University of Chicago, Chicago, IL 60637, USA

lightcurves, which extend up to 10–70 days, show no sign of the jet break that is expected in the standard framework of collimated outflows. We do so by showing that none of the X-ray afterglow lightcurves in our sample satisfies the relation between the spectral and temporal indices that is predicted for the phase after jet break. The jet break time can be predicted by inverting the tight empirical relation between the peak energy of the spectrum and the collimation-corrected energy of the prompt emission (the Ghirlanda relation). We find that there are no temporal breaks within the predicted time intervals in X-ray band. This requires either that the Ghirlanda relation has a larger scatter than previously thought, that the temporal break in X-rays is masked by some additional source of X-ray emission, or that it does not happen because of some unknown reason.

Subject headings: gamma rays: bursts — radiation mechanisms: non-thermal — ISM: jets and outflows

1. Introduction

The *Swift* satellite (Gehrels et al. 2004) has enabled the acquisition of early, dense, and detailed data on the X-ray afterglows of gamma-ray bursts (GRBs) (e.g., Burrows et al. 2005a; Tagliaferri et al. 2005; O'Brien et al. 2006). Analysis of X-ray telescope (XRT; Burrows et al. 2005b) data has revealed complex temporal behavior in the early phase of the afterglow (Nousek et al. 2006; Zhang et al. 2006; O'Brien et al. 2006). In addition to investigating the early phase of the X-ray afterglows, we can study the temporal and spectral properties of the X-ray afterglows at later times ($\gtrsim 10^4$ s), which had been studied mainly using optical data before the *Swift* era. It is widely believed that the GRBs arise from collimated outflows (i.e., jets). This picture is supported by the break from a shallower to a steeper slope that is observed in many afterglow light curves at around a day after the burst (Sari et al. 1999). These breaks are interpreted as being due to the geometrical effect caused by the inverse of the bulk Lorentz factor of the jet becoming larger than the physical opening angle of the jet, and to a hydrodynamical transition of the jet (i.e., a broadening of the jet), which is expected to occur shortly afterward. The break is therefore expected to be independent of wavelength (i.e., achromatic). Importantly, in the standard synchrotron-shock model (Sari et al. 1998), the observed flux above the cooling frequency does not depend on the density of ambient matter. Consequently, the X-ray afterglow is expected to be less variable than the optical one. Hence, observations of X-ray afterglows are a useful tool for studying the jet break.

In this paper, we investigate the presence or absence of a jet break in the X-ray afterglows of recent *Swift* GRBs. According to Frail et al. (2001) and Bloom et al. (2003), given the

observed jet break time, we can calculate the jet opening angle and thereby the collimation-corrected gamma-ray energy (E_γ). After correcting for the jet collimation, E_γ shows a tight correlation with the peak energy $E_{\mathrm{peak}}^{\mathrm{src}}$ of the νF_ν spectrum in the source-frame: $E_{\mathrm{peak}}^{\mathrm{src}} \propto E_\gamma^{0.7}$ (the Ghirlanda relation: Ghirlanda et al. 2004b). For *Swift* GRBs in which one can obtain both $E_{\mathrm{peak}}^{\mathrm{src}}$ and the isotropic-equivalent gamma-ray energy $E_{\mathrm{iso}} = E_\gamma / (1 - \cos\theta_{\mathrm{j}})$, where θ_{j} is the opening-half angle of the jet, the Ghirlanda relation can be inverted to predict the value of θ_{j}, and hence the jet break time. The X-ray afterglow can then be investigated to find out whether a jet break is present at the expected epoch. Hence, we can check the validity of the Ghirlanda relation found for pre-*Swift* bursts using mainly optical observations, and also the validity of the theory of the jet break established in the pre-*Swift* era.

2. Data Analysis

2.1. Data Selection

In order to be able to do the analysis described above, both prompt and afterglow data are necessary. Among the 10 *Swift* long GRBs with measured redshifts detected before July 2005, we find, for seven of them, either that the peak energy is hard to constrain or that the XRT light curve was not observed for long enough. We have thus selected the other three well-sampled bursts (GRB 050401, XRF 050416a, and GRB 050525a) for our study.

The prompt emission of GRBs has a spectrum that is well described by the Band function (Band et al. 1993). We calculate the "bolometric" isotropic-equivalent gamma-ray energy, E_{iso}, in the source frame by integrating the best-fit model for the time-averaged spectrum over the energy range 1–10^4 keV. In order to do this, it is necessary to know the overall shape of the spectrum, and therefore the three parameters of the Band function. In the cases of GRB 050525a and XRF 050416a, we find that the peak energy, $E_{\mathrm{peak}}^{\mathrm{obs}}$, of the gamma-ray spectrum falls within the energy range of *Swift* Burst Alert Telescope (BAT; 15–150 keV; Barthelmy et al. 2005). The Band function gives a significantly better fit than does a single power-law (PL) model or a power-law times exponential (PLE) model, and adequately describes the BAT spectral data for these two bursts. In the case of GRB 050401, $E_{\mathrm{peak}}^{\mathrm{obs}}$ falls outside the energy range of BAT. Since GRB 050401 was simultaneously observed (Golenetskii et al. 2005a) by Konus-Wind (20 keV–14 MeV; Aptekar et al. 1995), we utilize the Konus-Wind spectral data to find $E_{\mathrm{peak}}^{\mathrm{obs}}$.

Here we describe the results of the spectral and temporal analyses that we performed on the prompt emission and X-ray afterglow, of each burst. Table 1 gives the redshift, T_{90} duration, peak photon energy flux, and photon energy fluence determined from our analyses,

while Table 2 summarizes the best-fit spectral parameters for the prompt emission and the X-ray afterglow for each burst. Throughout this paper, we use HEAsoft 6.0, which includes the *Swift* software package (release 2005-08-08). We also adopt a cosmological model with $\Omega_{\rm m} = 0.3$, $\Omega_\Lambda = 0.7$, and $H_0 = 70$ kms^{-1}Mpc^{-1}. Errors quoted are at the 90% confidence level unless otherwise stated.

2.2. GRB 050401

GRB 050401 was detected and localized by the *Swift* BAT at 14:20:15 UTC on 2005 April 1 (Barbier et al. 2005). *Swift* autonomously slewed to the GRB position and the XRT found the X-ray afterglow emission at (R.A., Dec.) $= (16^{\rm h}31^{\rm m}28.85^{\rm s}, +02°11'14.4'')$ with the 90% error radius of $3.3''$ (Moretti et al. 2006). The optical afterglow emission was also detected with several ground observations (e.g., Rykoff et al. 2005). Fynbo et al. (2005) detected several absorption lines consistent with absorption systems at redshifts $z = 2.50$ and $z = 2.90$. Following these authors, we adopt $z = 2.90$.

We first analyze the *Swift* BAT data for the prompt emission. We subtracted the background using the modulations of the coded aperture mask (mask-weight technique). The prompt emission has a T_{90} duration of 34.3 s. The *Swift* BAT time-averaged spectral data in 15–150 keV is adequately fit by a single power-law model ($N(E) \propto E^{-\Gamma}$) and gives a photon index of $\Gamma = 1.54^{+0.07}_{-0.07}$ with $\chi^2_\nu = 0.73$ (58 dof). Neither the Band function nor the cut-off power-law model improves the fit significantly. We then analyzed the time-averaged spectral data from Konus-Wind, which has a wider energy range. We used the spectral data from an adjacent time domain to subtract the background from the spectral data during the burst. We then fit to the data a power-law (PL) model, a power-law times exponential model (PLE) and a Band function: $N(E) \propto E^{\alpha_{\rm B}} \exp(-\frac{E}{E_0})$ for $E < (\alpha_{\rm B} - \beta_{\rm B})E_0$; $\propto E^{\beta_{\rm B}}$ for $E \geq (\alpha_{\rm B} - \beta_{\rm B})E_0$, where $\nu F(\nu)$ peaks at $E_{\rm peak}^{\rm obs} = (\alpha_{\rm B} + 2)E_0$. We find $\chi^2_\nu = 2.38$ (58 dof), $\chi^2_\nu = 1.12$ (57 dof), and $\chi^2_\nu = 1.00$ (56 dof), respectively. Thus the spectral data strongly requests the Band function over the PL and PLE models. The best fit values and uncertainties for the Band function parameters obtained in this way are $E_{\rm peak}^{\rm obs} = 115^{+19}_{-16}$ keV, $\alpha_{\rm B} = -0.87^{+0.36}_{-0.27}$, and $\beta_{\rm B} = -2.47^{+0.21}_{-0.36}$, respectively. Using the redshift $z = 2.90$, the peak energy at the rest frame of the GRB is determined as $E_{\rm peak}^{\rm src} = 447^{+75}_{-64}$ keV, and the isotropic energy as $E_{\rm iso} = 3.43^{+0.37}_{-0.34} \times 10^{53}$ erg over 1 keV to 10 MeV.

We next analyze the *Swift* XRT data for the event. The XRT acquired data mainly in Windowed Timing (WT) mode in the first ~ 10000 s from the BAT trigger, and then switched to Photon Counting (PC) mode according to the source count rate. We used XSELECT to extract source and background counts from the cleaned event list (0.5–10.0

keV), using the standard grade selections of 0–12 for PC mode data, and of 0–2 for WT mode data. We calculate the source light curve and spectrum from a region with a length of $80''$ in uncompressed direction for WT mode, and a circular region with a radius of $47''$ for PC mode. We extract the background light curves and spectra from outer regions, excluding other X-ray sources that are visible in the XRT image. We converted the count rate to the unabsorbed flux in the 2–10 keV energy band using the best fit spectral model.

Fig. 1 shows the background-subtracted 2–10 keV light curve. The X-ray afterglow of GRB 050401 faded slowly with a very shallow temporal index in the time interval from T+134 s to T+2484 s. Here, T represents the trigger time of the BAT. Extrapolating the initial slope to late times, the WT data in T+7414 s – T+8274 s and the PC mode data in T+13486 s – T+14066 s clearly have lower fluxes than expected. The XRT also detected the fading afterglow at a later time between T+4.4 days and T+ 7.2 days. Including these data points, the best fit to the overall light curve is given by a broken power-law model: $F(t) \propto t^{\alpha_1}$ for $t < t_{\rm b}$; $\propto t^{\alpha_2}$ for $t \geq t_{\rm b}$. The best-fit model gives $\chi^2_\nu = 1.59$ (29 dof), with best-fit parameters $\alpha_1 = -0.57 \pm 0.02$, $\alpha_2 = -1.34 \pm 0.05$ and $t_{\rm b} = 5390 \pm 450$ s. This result is consistent with that of De Pasquale et al. (2006). We have also analyzed the spectral data before and after the temporal break. We find that both spectra are well-fit by a power-law model. The best-fit model requests more absorption than the value $N_{\rm H} = 4.9 \times 10^{20}$ cm^{-2} expected for the galaxy alone. We have therefore added absorption at the redshift of the GRB ($z = 2.90$) to the model. The best-fit parameters are $\Gamma = 2.03^{+0.05}_{-0.05}$ and $N^z_{\rm H} = 3.7^{+0.5}_{-0.5} \times 10^{22}$ cm^{-2} ($\chi^2_\nu = 1.15$ (241 dof)) prior to the break, and $\Gamma = 1.98^{+0.26}_{-0.24}$ and $N^z_{\rm H} = 3.0^{+3.1}_{-2.5} \times 10^{22}$ cm^{-2} ($\chi^2_\nu = 0.65$ (22 dof)) after the break. There is therefore no significant evidence for evolution of the spectral shape from before the break to after it, taking into account the uncertainties in the spectral parameters.

2.3. XRF 050416a

The X-ray flash, XRF 050416a, was detected and localized by the *Swift* BAT at 11:04:44.5 UTC on 2005 April 16 (Sakamoto et al. 2005). *Swift* autonomously slewed to the GRB position and *Swift* XRT found the X-ray afterglow emission at (R.A., Dec.) = ($12^{\rm h}33^{\rm m}54.63^{\rm s}$, $+21°03'27.3''$) with the 90% error radius of $3.3''$ (Moretti et al. 2006). The detailed analysis of the BAT, XRT and UVOT data are reported in several papers (BAT; Sakamoto et al. (2006a), XRT; Mangano et al. (2006), UVOT; Holland et al. (2006)). The spectrum of the host galaxy of XRF 050416a was obtained using the 10 m Keck I telescope; the host galaxy is faint and blue with a high star formation rate and its redshift is $z = 0.6535 \pm 0.0002$ (Cenko et al. 2005).

The prompt emission had a duration of $T_{90} = 2.4$ s. XRF 050416a is the softest burst observed by *Swift* BAT as of July 2005. Sakamoto et al. (2006a) showed that the time-averaged spectrum is much steeper than the photon index of $\Gamma = 2$, indicating the spectral peak lies at the lower end of or below the BAT energy range. Following these authors, we adopt the Band function model with a fixed $\alpha_B = -1$, which is the typical value for BATSE GRBs (Kaneko et al. 2006). The fit gives $E_{\text{peak}}^{\text{obs}} = 18.0^{+3.9}_{-2.9}$ keV. In order to take into account the uncertainty in the low energy photon index, which may affect the total isotropic energy, E_{iso}, we have performed spectral fits to the *Swift* BAT spectral data, varying α_B from -1.5 to -0.67. These limits correspond to the indices predicted for a spectrum in the fast cooling phase; i.e., with $\nu_c < \nu < \nu_m$ and $\nu < \nu_c$, respectively (Sari et al. 1998). Here, ν_c is the synchrotron cooling frequency and ν_m is the synchrotron frequency of electrons with the minimum energy. We then find the best-fit values of the Band function parameters and their uncertainties to be $E_{\text{peak}}^{\text{obs}} = 17.3^{+3.0}_{-8.0}$ keV and $\beta_B < -3.35$ with $\chi^2_\nu = 0.80$ (56 dof). Using the observed redshift of $z = 0.6535$, we find $E_{\text{peak}}^{\text{src}} = 28.5^{+5.0}_{-13.2}$ keV, and $E_{\text{iso}} = 8.3^{+6.5}_{-1.3} \times 10^{50}$ erg.

The XRT data were acquired in PC mode throughout the observation. We extracted the light curves and spectra from the data in a circular region with a radius of $47''$. The data obtained in PC mode sometimes suffered from pile-up, especially when the count rate was higher than 0.5 counts/s (Nousek et al. 2006). For this burst, the XRT count rate exceeded this limit for the first ~ 500 s of the observation. From image analysis, we find the central region with radius of $6''$ deviates from the XRT point spread function. We therefore excluded the events in this region when we derived the source light curve and spectrum for the time interval T+94 – T+596 s; we used the full region of the circle with radius of $47''$ in the later period. The effective area was corrected using the calibration data and the *FTOOL* xrtmkarf.

Fig. 2 shows the background-subtracted 2–10 keV light curve The light curve is well fit by a broken power-law with $\chi^2_\nu = 1.12$ (32 dof). There is an indication of a break in the light curve at $t_b = 1670 \pm 600$ s, which is also reported by Nousek et al. (2006). The decay index is $\alpha_1 = -0.55 \pm 0.06$ before the break and $\alpha_2 = -0.82 \pm 0.03$ after it. Strikingly, the light curve shows a shallow decay extending to ~ 74.5 days after the trigger. The spectral data before and after the break are both well fit by a power-law model with galactic absorption ($N_H = 3.4 \times 10^{20}$ cm^{-2}) and an additional absorption component at the redshift of the GRB (z= 0.6535). The best-fit parameters are $\Gamma = 2.20^{+0.27}_{-0.24}$ and $N_H^z = 7.3^{+3.7}_{-3.2} \times 10^{21}$ cm^{-2} ($\chi^2_\nu = 1.38$ (20 dof)) before the break, and $\Gamma = 2.04^{+0.16}_{-0.15}$ and $N_H^z = 5.5^{+2.2}_{-1.9} \times 10^{21}$ cm^{-2} ($\chi^2_\nu = 0.93$ (64 dof)) after the break. Thus, there is no significant evidence for spectral evolution, after taking into account the uncertainties in the spectral parameters.

2.4. GRB 050525a

GRB 050525a was a very bright GRB that was detected and localized by the *Swift* BAT at 00:02:52.8 UTC on 2005 May 25 (Band et al. 2005). *Swift* autonomously slewed to the GRB position, and *Swift* XRT and UVOT started their observations about 100 s after the trigger, and both found a fading source. The optical coordinates are (R.A., Dec.) = $(18^{\mathrm{h}}32^{\mathrm{m}}32.62^{\mathrm{s}}, +26°20'21.6'')$ with an estimated uncertainty of $0.2''$. (Blustin et al. 2006). Foley et al. (2005) used GMOS on the Gemini-North telescope to obtain an optical spectrum of the burst and reported that the redshift of the host galaxy is $z = 0.606$ based on [O III] 5007 and H beta emission and Ca H&K and Ca I 4228 absorption.

The prompt emission had a duration of $T_{90} = 8.9$ s. We fit the *Swift*-BAT time-averaged spectral data using a power-law (PL) model, a power-law times exponential model (PLE) and a Band function. We find $\chi_\nu^2 = 3.30$ (58 dof), $\chi_\nu^2 = 0.26$ (57 dof), and $\chi_\nu^2 = 0.27$ (56 dof). Thus both the PLE model and the Band function are acceptable. We here employ the Band function to constrain the upper limit on the higher energy index (β_{B}) and adequately include the uncertainty into the calculation of E_{iso}. The Band function fit to the *Swift* BAT time-averaged spectrum in 15–150 keV gives best-fit parameters $E_{\mathrm{peak}}^{\mathrm{obs}} = 78.2_{-1.6}^{+4.7}$ keV, $\alpha_{\mathrm{B}} = -0.97_{-0.10}^{+0.11}$ and $\beta_{\mathrm{B}} < -2.55$. Using the observed redshift of $z = 0.606$, we find $E_{\mathrm{peak}}^{\mathrm{src}} = 125.6_{-2.6}^{+7.6}$ keV, and $E_{\mathrm{iso}} = 2.23_{-0.11}^{+0.03} \times 10^{52}$ erg.

The X-ray afterglow was very bright just after the trigger. Hence, the observation was made first in Photo-Diode (PD) mode and was switched to PC mode after T+5859 s. No WT data were taken because of engineering tests that were being performed at the time of the burst. Since we cannot eliminate photons from the calibration source in PD mode, we use PD data in the 0.5-4.5 keV band, while we use PC data in 0.5–10.0 keV. Fig. 3 shows the background subtracted 2–10 keV light curve. We extrapolated the spectrum in PD mode to the wider band when making the light curve. The last 2 points (T+10.0 days – T+35.0 days) are not considered in Blustin et al. (2006) whose result for < T+5.4 days is consistent with ours. In the time interval from T+280 s to T+1048 s, we can see an excess above the fitted line. Following Blustin et al. (2006), we identify the excess with a weak flare. If we fit the data excluding the flare regime and the last upper limit, a broken power-law model gives $\chi_\nu^2 = 0.54$ (27 dof), with best fit parameters $\alpha_1 = -1.18 \pm 0.02$, $\alpha_2 = -1.51 \pm 0.06$ and $t_{\mathrm{b}} = 10600 \pm 3300$ s. The spectral data before and after the break are extracted from the entire PD data and the PC data after break, respectively. Both spectra are well fit by a power-law model with a galactic absorption ($N_{\mathrm{H}} = 9.1 \times 10^{20}$ cm^{-2}) and an additional absorption at the redshift of the GRB (z= 0.606). The best-fit parameters are $\Gamma = 1.92_{-0.05}^{+0.05}$ and $N_{\mathrm{H}}^z = 2.6_{-0.4}^{+0.4} \times 10^{21}$ cm^{-2} ($\chi_\nu^2 = 1.09$ (271 dof)) before the break, and $\Gamma = 2.11_{-0.39}^{+0.28}$ and $N_{\mathrm{H}}^z = 1.5_{-1.5}^{+3.6} \times 10^{21}$ cm^{-2} ($\chi_\nu^2 = 0.79$ (22 dof)) after the break. Thus, there is no significant

evidence for spectral evolution, after taking into account the uncertainties in the spectral parameters.

3. Results and Discussion

3.1. Investigation of Jet Break Features

Spectral parameters of the prompt emission are well constrained by the *Swift* BAT and Konus data plus the optically determined redshifts. Fig. 4 shows the locations of GRBs in the $(E_{\rm iso}, E_{\rm peak}^{\rm src})$-plane, where $E_{\rm iso}$ is the isotropic-equivalent energy and $E_{\rm peak}^{\rm src}$ is the peak energy of the burst spectrum in the rest frame of the burst. The burst locations previously reported by Ghirlanda et al. (2004b) are shown as filled gray circles. The dashed and dot-dashed lines are the correlations between $E_{\rm iso}$ and $E_{\rm peak}^{\rm src}$ reported by Amati et al. (2002) and Ghirlanda et al. (2004b), respectively. The locations of XRF 050416a, GRB 050525a, and GRB 050401, derived from Swift and Konus-Wind observations, lie within the scatter of the Amati relation ($E_{\rm peak}^{\rm src} \propto E_{\rm iso}^{0.5}$: Amati et al. 2002). Although it has been suggested that the Amati relation may have a large intrinsic scatter [Nakar & Piran (2005); Band & Preece (2005), but see Ghirlanda et al. (2005); Bosnjak et al. (2005)], the locations of the three bursts discussed in this paper lie close to the best-fit relations derived by Amati et al. (2002) and Ghirlanda et al. (2004b).

The X-ray follow-up observations for the three bursts start at $\sim$T+100 s and end at T+12.4 – T+74.5 days. The X-ray afterglow light curves do not exhibit a steep decline at the beginning of the observations, although Mangano et al. (2006) and O'Brien et al. (2006) show that a fairly steep early decline can be seen for XRF 050416A by combining BAT data with XRT image mode and low rate mode data. The light curves show breaks at an early epoch, $t_{\rm b} \sim 10^3$–10^4 s which is similar to the behavior seen in the X-ray afterglow of other bursts (Nousek et al. 2006; O'Brien et al. 2006). The decay slopes after the breaks are shallower than the $\propto t^{-2}$ behavior expected after the jet-break (Sari et al. 1999; Dai & Cheng 2001).

We first consider the behavior of the X-ray afterglows of the three bursts within the framework of the standard afterglow model in the pre-*Swift* era. The jet decelerates rapidly after the sideways expansion becomes significant, and the external shock enters the slow-cooling phase (Sari et al. 1998). For example, if the the cooling frequency lies below the X-ray band (i.e., $\nu > \nu_{\rm c}$), the temporal decay index (α) and the energy spectral index ($\beta = -\Gamma + 1$) after the jet break are given by $\alpha = -p$ and $\beta = -p/2$, respectively. Here, $p > 2$ is the power-law index of the electron energy distribution (Sari et al. 1999). Eliminating p, gives a

relation between α and β (the so called α–β relation): $\alpha = 2\beta$. If $1 < p < 2$, the α–β relation takes a different form: $\beta = 2\alpha + 3$ (Dai & Cheng 2001). Similar formulae exist when the cooling frequency lies above the X-ray band (i.e., $\nu_\mathrm{m} < \nu < \nu_\mathrm{c}$) but this is likely to be true only at early times. The observed results for the three bursts are shown in Fig. 5 together with the theoretical predictions of the $\alpha - \beta$ relations before and after the jet break, shown as dashed and dotted lines respectively. It is clear that none of the observed data points is consistent with the theoretical prediction of the standard afterglow models after the jet break.

For each of the three events, we find no clear evidence of a jet break in the X-ray light curve earlier than 10^6 sec after the trigger. We therefore invert the Ghirlanda relation to predict the jet break time for each of the three bursts that makes them satisfy the $E_\mathrm{peak}^\mathrm{src}$–$E_\gamma$ relation. The Ghirlanda relation is (Ghirlanda et al. 2004b)

$$E_\mathrm{peak}^\mathrm{src} = A E_{\gamma,52}{}^{0.706} \quad , \tag{1}$$

where $E_\gamma = (1 - \cos\theta_\mathrm{j})E_\mathrm{iso}$ is the collimation-corrected energy and θ_j is the opening half-angle of the jet. Here we define $E_{\gamma,52} = E_\gamma/10^{52}$ erg. The relation is based on the jet breaks observed mainly in the optical band. However, the jet break should appear in the X-ray band at the same time that it appears in the optical band because the break is geometrical and hydrodynamical in origin. Fig. 6 shows the correlation between E_γ and $E_\mathrm{peak}^\mathrm{src}$ for the GRB samples in Ghirlanda et al. (2004b). The left and right diagonal lines in the figure are for $A = 4380$ keV and $A = 1950$ keV, respectively; the band between the two lines includes all of the central values of the locations of GRBs with well-constrained properties in the Ghirlanda et al. (2004b) samples. The expression for the jet break time is (Sari et al. 1999)

$$t_\mathrm{jet} = 130 \, \theta_\mathrm{j}^{8/3}(1+z)\left(\frac{n\eta_\gamma}{E_\mathrm{iso,52}}\right)^{-1/3} \quad \text{days,} \tag{2}$$

where $E_\mathrm{iso,52}$, n, η_γ, and z are respectively the isotropic-equivalent energy in units of 10^{52} erg, the number density of the ambient (uniform) medium, the efficiency of the shock in converting the energy in the ejecta into γ-rays, and the source redshift. Using Eqs. (1) and (2), we obtain

$$t_\mathrm{jet} = 389 \, (1+z)\left(\frac{n}{3 \text{ cm}^{-3}}\right)^{-1/3}\left(\frac{\eta_\gamma}{0.2}\right)^{-1/3} E_\mathrm{iso,52}^{-1}\left(\frac{E_\mathrm{peak}^\mathrm{src}}{A}\right)^{1.89} \quad \text{days.} \tag{3}$$

Using this equation, we can calculate t_jet from the $E_\mathrm{peak}^\mathrm{src}$ and E_iso values we have derived from the observations. The efficiency η_γ of the shock, and especially, the number density n of the ambient medium, are poorly known for most bursts. In particular, n could easily lie anywhere in a fairly wide range, where the majority are within $1 < n < 30$ cm^{-3} (Panaitescu & Kumar 2001, 2002).

Following the assumption made by Ghirlanda et al. (2004b) for most of their samples, we initially assume $n = 3$ cm^{-3} and $\eta_\gamma = 0.2$. Allowing A to vary from 1950 keV to 4380 keV in Eq. (3) then gives the time interval in which the jet break is expected to occur if the Ghirlanda relation is satisfied, assuming these values of n and η_γ (or equivalently, that $n\eta_\gamma = 0.6$). Allowing n to vary between $1 - 30$ cm^{-3} (or equivalently, $0.2 < n\eta_\gamma < 6$), in Eq. (3) gives the time interval in which the jet break is expected to occur if the Ghirlanda relation is satisfied without assuming a particular value of $n\eta_\gamma$. The intervals thus obtained are also plotted in Fig. 1–3. The dash-dotted, dashed, and solid lines show the allowed time intervals, without assuming a particular value of $n\eta_\gamma$ and taking into account the errors in $E_{\rm iso}$ and $E_{\rm peak}^{\rm src}$; assuming a particular value of $n\eta_\gamma$ and taking into account the errors in $E_{\rm iso}$ and $E_{\rm peak}^{\rm src}$; and assuming a particular value of $n\eta_\gamma$ without taking into account the errors in $E_{\rm iso}$ and $E_{\rm peak}^{\rm src}$. The time interval in which the jet break is expected to occur was completely observed for XRF 050416a and GRB 050525a, but no temporal break is seen within the interval. The break at about 11000 sec for GRB 050525a, which is close to the edge of the expected time interval, was suggested to be a possible jet break because of its achromatic feature between X-ray and optical bands (Blustin et al. 2006). However, if we consider the discrepancy in the spectral and temporal relations with the theoretical predictions as well, it is suggested that the break is not a jet break. For GRB 050401, time intervals on both sides of the time interval were observed and can be joined with a single power-law decay. Thus, none of the three bursts exhibit a jet break within the time period required if they are to satisfy the Ghirlanda relation.

We now consider the implications if the jet break occurs at either an earlier or a later epoch than the expected time interval. If we assume that the break at $t_{\rm b}$ corresponds to the jet break time, the temporal decay indices are inconsistent with the values predicted by the standard afterglow model, as already discussed. In addition, the values of $\theta_{\rm j}$ are smaller than their values for other bursts. If we assume, on the other hand, that the jet break occurs after the time interval covered by the Swift XRT observations, we can derive a lower limit on $\theta_{\rm j}$, and hence on E_γ, from the last time at which the afterglow was detected. Fig. 6 shows that in this case the three bursts are also outliers of the Ghirlanda relation. Reconciling the X-ray afterglow light curve observed for these three bursts with the standard afterglow model requires very unusual values of n and/or η_γ. In order to derive from Eq. 3 a jet break time that corresponds to $t_{\rm b}$, the product of n and η_γ must be around 200, 50 and 10 for GRB 050401, XRF 050416a, and GRB 050525a, respectively. In order to derive from Eq. 3 a jet break time that is later than the last detections, the product of n and η_γ should be smaller than 0.2, 2×10^{-4} and 2×10^{-3} for the three bursts, respectively (see also Levinson & Eichler 2005).

For 18 GRBs detected in the pre-*Swift* era, Liang & Zhang (2005) found a tight cor-

relation among $E_{\rm peak}^{\rm src}$, $E_{\rm iso}$, and the rest-frame jet break time $t_{\rm jet}^{\rm src}$ (see also Xu 2005). The Liang-Zhang relation is model-independent, while the Ghirlanda relation is not because the jet opening angle is estimated using the standard jet model of the afterglow. If the optical breaks discussed in Liang & Zhang (2005) are jet breaks, the Liang-Zhang relation is equivalent to the Ghirlanda relation (Liang & Zhang 2005; Xu 2005; Nava et al. 2006). We have shown here that if we apply a theory of achromatic jet break in the afterglow that was used in the pre-*Swift* era, the three *Swift* GRBs we have analyzed are outliers of the Ghirlanda relation. Therefore, these three *Swift* bursts are also outliers of the Liang-Zhang relation if the optical breaks discussed in Liang & Zhang (2005) are jet breaks. In fact, the rest-frame jet break time $t_{\rm jet}^{\rm src}$ can be predicted using the Eq. (5) of Liang & Zhang (2005) and the values of $E_{\rm peak}^{\rm src}$ and $E_{\rm iso}$ that we have derived from the observations. The derived values of $t_{\rm jet}^{\rm src}$ for the three events are $1 - 2$ days after the bursts in the observer frame. However, no break is visible at that epoch in the light curves of X-ray afterglows.

Up to now, we have assumed that the ambient density is uniform. However, Nava et al. (2006) have investigated the case of a wind profile (i.e., $n \propto r^{-2}$) and find that E_γ is again tightly correlated with $E_{\rm peak}^{\rm src}$. Since this Ghirlanda-wind correlation is also equivalent to the Liang-Zhang relation (Nava et al. 2006), the three *Swift* GRBs discussed in this paper are also outliers of the Ghirlanda-wind relation.

3.2. Implications of no Jet Break Feature in the X-ray Band

As discussed in the previous subsection (§3.1), we find that, for the three bursts we consider, the empirically derived Ghirlanda relation is incompatible with the standard jet model of GRB afterglows that worked well prior to *Swift*. This may be because prior to *Swift* jet breaks were observed mainly in the optical band, whereas in this paper, we have investigated the presence or absence of jet breaks in the X-ray band. We consider two possible ways of reconciling this discrepancy.

One possibility is that the jet break takes place in the optical band at the time expected from the Ghirlanda relation, even for the three bursts that we have studied, but that it is masked in the X-ray band by one or more sources of additional emission, such as (1) inverse Compton emission, (2) emission from a cocoon around the jet, (3) emission from the external shock as it passes through a dense region in the surrounding medium, (4) continuous injection of energy into the external shock producing a separate source of X-ray emission, or (5) a separate jet component (Panaitescu et al. 2006). If one or more additional components contribute to the X-ray afterglow emission, one might expect the observed afterglow to exhibit bumps and/or dips. However, the observed lightcurves of the X-ray afterglows for

the three bursts all exhibit a rather simple power-law decay. This, plus the fact that the decay slopes of the X-ray afterglows of the three bursts that we consider are shallower both before the observed break and after than in the cases of many of the light curves of optical afterglows observed prior to *Swift*, favors the possibility that energy is being continuously injected into the external shock and the X-ray emission resulting from this injection of energy masks the jet break in X-ray band that is associated with the jet break in the optical band.

A second possibility is that the jet break occurs at a later time compared to the time it occurs in previous samples of GRBs. If this is case, many *Swift* GRBs would have to belong to a different class of events from those detected by previous missions, such as *CGRO* BATSE, *RXTE*, *BeppoSAX* and *HETE-2*, and it would imply that the Ghirlanda relation has a larger scatter than previously thought. It is difficult to assess observational selection effects, given the limited number of *Swift* GRBs for which $E_{\rm iso}$ and $E_{\rm peak}^{\rm src}$ are known as of July 2005. However, the properties of the prompt emission of the three bursts that we consider here are indistinguishable from those of bursts detected prior to *Swift*, and their values of $E_{\rm peak}^{\rm src}$ and $E_{\rm iso}$ satisfy the Amati relation, making the possibility that many *Swift* GRBs belong to a different class of events from those detected by previous missions seem unlikely.

It is also possible that both scenarios occur in different bursts. Simultaneous X-ray and optical observations of GRB afterglows around the expected jet break time could distinguish between these two possibilities. In the former scenarios, a jet break at the expected time should be seen in the optical band but not in the X-ray band, while in the latter scenario, a jet break should not be seen in either the optical band or the X-ray band.

Current observational evidence is limited and ambiguous. In the case of GRB 050401, Panaitescu et al. (2006) report that the optical lightcurve extends to ~ 10 days without a break. This period covers the entire time interval during which a jet break is expected, if the burst satisfies the Ghirlanda relation. Therefore, either version (5) of the former scenario, in which the X-ray and the optical afterglows are due to separate jet components, or the latter scenario are preferable for this event. A recent Swift burst, GRB 060206, showed a late-time steepening of the optical light curve, but no break in the X-ray light curve at the same time (Monfardini et al. 2006), which also lends support to version (5) of the former scenario, in which the X-ray and the optical afterglows are due to separate jet components.

In the case of XRF 050416a, there are no observations of the afterglow in the optical band in the expected time interval. However, the decay slope of the afterglow lightcurve of XRF 050416a in X rays is shallow out to 75 days after the burst (Levan et al. 2006; Hullinger et al. 2006). The X-ray afterglows of XRF 020427 (Amati et al. 2004) and XRF 050215b (Sakamoto et al. 2006b) are also shallow out to very late times. The properties of the prompt emission and the shallow decay slopes of the X-ray afterglows imply that, in the

cases of these two bursts, the fluence in the afterglow is comparable to, or may even exceed, that in the prompt emission (see also O'Brien et al. 2006). This suggests that the efficiency of the prompt emission may be relatively small, and provides support for the possibility that energy is being continuously injected into the external shock, and delays the jet break in X rays beyond the time of the last XRT observations (Sakamoto et al. 2006b). It also is conceivable that continuous energy injection into the external shock could power X-ray emission that masks the usual jet break in X-rays.

In the case of GRB 050525a, *Swift* UVOT in six different filters (V, B, U, UVW1, UVM2, UVW2) from ∼T+70 to ∼T+50000 s (Blustin et al. 2006). However, only upper limits are available in all the bands after ∼T+50000 s, which unfortunately lies in the middle of the time interval in which the jet break is expected to occur. After the source had faded below the detection limit of UVOT, there are detections in unfiltered light after ∼ 10^5 s. However, those observations are not sufficient to determine if there is a break or not.

The lack of an observed jet break in the X-ray afterglows of the three bursts we consider here also has implications for the use of GRBs for cosmological studies. It has been suggested that the tightness of the Ghirlanda relation, as reported prior to our study, makes it possible to use GRBs as "standard candles" for constraining the properties of dark energy (Ghirlanda et al. 2004a). Our results suggest additional caution in using the Ghirlanda relation for this purpose.

Given the importance of the presence or absence of a jet break for understanding the nature of GRB jets and for the use of GRBs as "standard candles" for cosmology, we strongly encourage simultaneous X-ray and optical observations of GRB afterglow around the expected jet break time for GRBs having reliable measurements of E_{peak}^{obs} and redshifts in order to investigate whether the breaks seen in the optical are accompanied by breaks in the X-ray at the time expected in the standard jet model of GRB afterglows.

REFERENCES

Amati, L., et al. 2002, A&A, 390, 81

Amati, L., et al. 2004, ASPC, 312, 189

Aptekar, R., et al. 1995, Space Sci. Rev., 71, 265

Band, D. L., et al. 1993, ApJ, 413, 281

Band, D. L. & Preece, R. D. 2005, ApJ, 627, 319

Band, D. L., et al. 2005, GCN Circ. 3466

Barbier, L., et al. 2005, GCN Circ. 3162

Barthelmy, S., et al. 2005, Sp. Sci. Rev., 120, 143

Bloom, J. S., Frail, D. A., Kulkarni, S. R. 2003, ApJ, 594, 674

Blustin, A. J., et al. 2006, ApJ, 637, 901

Bosnjak, Z., et al. 2005, submitted to MNRAS (astro-ph/0502185)

Burrows, D. N., et al. 2005a, Science, 309, 1833

Burrows, D. N., et al. 2005b, Sp. Sci. Rev., 120, 165

Cenko, S. B., et al. 2005, GCN Circ. 3542

Chincarini, G., et al. 2005, submitted to ApJ (astro-ph/0506453)

Dai, Z. G. & Cheng, K. S. 2001, ApJ, 558, L109

De Pasquale, M. et al. 2006, MNRAS, 365, 1031

Foley, R. J., et al. 2005, GCN Circ. 3483

Fynbo, J. P. U., et al. 2005, GCN Circ. 3176

Frail, D. A., et al. 2001, ApJ, 562, L55

Frontera, F. 2003, Lecture Notes in Physics, 598, ed. K. Weiler

Gehrels, N., et al. 2004, ApJ, 611, 1005

Ghirlanda, G., Ghisellini, G., Lazzati, D., & Firmani, C. 2004a, ApJ, 613, L13

Ghirlanda, G., Ghisellini, G., & Lazzati, D. 2004b, ApJ, 616, 331

Ghirlanda, G., Ghisellini, G., & Firmani, C. 2005, MNRAS, 361, L10

Golnetskii, S., et al. 2005a, GCN Circ. 3179

Golnetskii, S., et al. 2005b, GCN Circ. 3474

Holland, S. T., et al. 2006, astro-ph/0604316

Hullinger, A., et al. 2006, ApJ, to be submitted

Kaneko, Y., et al. 2006 ApJS, 166, 298

Kennea, J. A., et al. 2005, GCN Circ. 3268

Klotz, A., et al. 2005, A&A, 439, L35

Levan, A., et al. 2006, in preparation

Levinson, A. & Eichler, D. 2005, ApJ, 629, L13

Liang, E. W. & Zhang, B. 2005, ApJ, 633, 611

Mangano, V., et al. 2006, ApJ, accepted (astro-ph/0603738)

Monfardini, A. et al. 2006, astro-ph/0603181

Moretti, A., et al. 2006, A&A Letters, 448, L9

Nakar, E. & Piran, T. 2005, MNRAS, 360, L73

Nava, L., et al. 2006, A&A, 450, 471

Nousek, J. A., et al. 2006, ApJ, 642, 389

O'Brien, P. T., et al. 2006, ApJ, 647, 1213

Panaitescu, A. & Kumer, P. 2001 ApJ, 560, L49

Panaitescu, A. & Kumer, P. 2002 ApJ, 571, 779

Panaitescu, A., et al. 2006, MNRAS, 369, 2059

Rykoff, E. S., et al. 2005, ApJ, 631, L121

Sakamoto, T., et al. 2005, GCN Circ. 3264

Sakamoto, T., et al. 2006a, ApJ, 636, L73

Sakamoto, T., et al. 2006b, ApJ, to be submitted

Sari, R., Piran, T., & Narayan, R. 1998, ApJ, 497, L17

Sari, R., Piran, T., & Halpern, J. P. 1999, ApJ, 519, L17

Tagliaferri, G. et al. 2005, Nature, 436, 985

Xu, D. 2005, astro-ph/0504052

Zhang, B., et al. 2006, ApJ, 642, 354

Table 1.   Redshifts, durations, and emission properties of three *Swift* GRBs

GRB	redshift	T_{90} [s]	Peak 1 s Flux in 15-150 keV [erg cm^{-2} s^{-1}]	Fluence in 15-150 keV [erg cm^{-2}]	Observing Instruments
050401	2.9	34.3	$9.26^{+0.72}_{-0.72} \times 10^{-7}$	$8.49^{+0.32}_{-0.32} \times 10^{-6}$	*Swift* BAT, *Swift* XRT, VLT, Optical, ROTSE, Siding Spring
050416a	0.65	2.4	$2.02^{+0.20}_{-0.20} \times 10^{-7}$	$3.36^{+0.34}_{-0.32} \times 10^{-7}$	*Swift* BAT, *Swift* XRT, Keck
050525a	0.606	8.9	$3.62^{+0.06}_{-0.06} \times 10^{-6}$	$1.62^{+0.2}_{-0.02} \times 10^{-5}$	*Swift* BAT, *Swift* XRT, *Swift* UVOT, VLA INTEGRAL, Spitzer, HST, Numerous Optical & NIR

Table 2.   Prompt emission spectral parameters and X-ray afterglow temporal and spectral parameters

GRB	$\alpha_{\rm B}$	$\beta_{\rm B}$	$E^{\rm obs}_{\rm peak}$ [keV]	$E^{\rm src}_{\rm peak}$ [keV]	$E_{\rm iso}$ [10^{52} erg]	$t_{\rm b}$ [s]	α_1	α_2	Γ_1	Γ_2
050401	$-0.87^{+0.36}_{-0.27}$	$-2.47^{+0.21}_{-0.36}$	115^{+19}_{-16}	447^{+75}_{-64}	$34.3^{+3.7}_{-3.4}$	5390 ± 450	-0.57 ± 0.02	-1.34 ± 0.05	$2.03^{+0.05}_{-0.05}$	$1.98^{+0.26}_{-0.24}$
050416a	-	< -3.35	$17.3^{+3.0}_{-8.0}$	$28.5^{+5.0}_{-13.2}$	$0.083^{+0.065}_{-0.013}$	1670 ± 600	-0.55 ± 0.06	-0.82 ± 0.02	$2.20^{+0.27}_{-0.24}$	$2.04^{+0.16}_{-0.15}$
050525a	$-0.97^{+0.11}_{-0.10}$	< -2.55	$78.2^{+4.7}_{-1.6}$	$125.6^{+7.6}_{-2.6}$	$2.23^{+0.03}_{-0.11}$	10600 ± 3300	-1.18 ± 0.02	-1.51 ± 0.06	$1.92^{+0.05}_{-0.05}$	$2.11^{+0.28}_{-0.39}$

Note. — $\alpha_{\rm B}$, $\beta_{\rm B}$, $E^{\rm obs}_{\rm peak}$ and $E^{\rm src}_{\rm peak}$ are the parameters of the Band function. $E_{\rm iso}$ is calculated in 1–10^4 keV. $t_{\rm b}$ is break time observed in X-ray band. α_1 and α_2 are decay indices of the X-ray afterglows before and after $t_{\rm b}$. Γ_1 and Γ_2 are photon indices of the X-ray afterglows before and after $t_{\rm b}$.
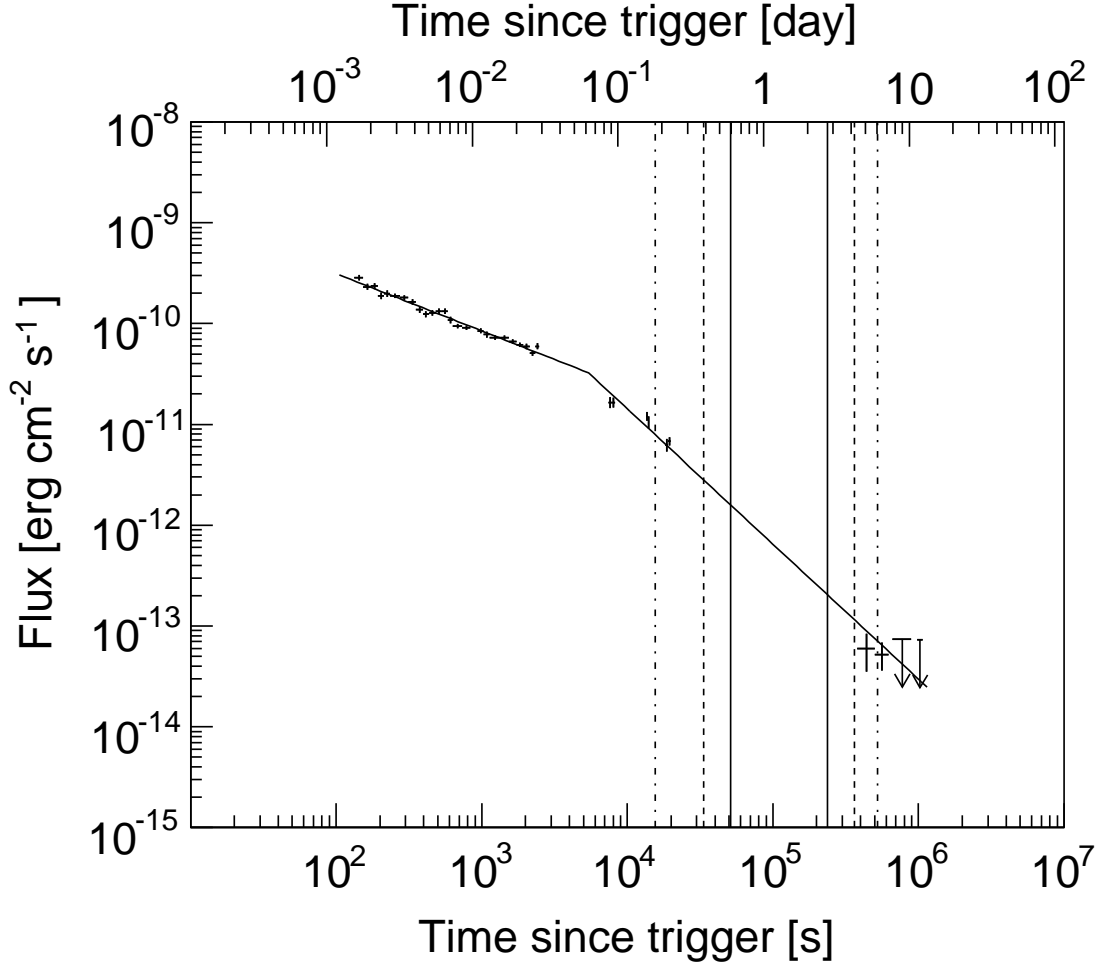
Fig. 1.— X-ray afterglow light curve of GRB 050401 in the 2–10 keV energy band. In order to satisfy the Ghirlanda relation between $E_{\mathrm{peak}}^{\mathrm{src}}$ and E_γ, the X-ray light curve should exhibit a jet break within the time interval indicated by the vertical lines. The dash-dotted, dashed, and solid lines show, respectively, the allowed time intervals, without assuming a particular value of $n\eta_\gamma$ and taking into account the errors in E_{iso} and $E_{\mathrm{peak}}^{\mathrm{src}}$ in Eq. 3; assuming a particular value of $n\eta_\gamma$ and taking into account the errors in E_{iso} and $E_{\mathrm{peak}}^{\mathrm{src}}$; and assuming a particular value of $n\eta_\gamma$ without taking into account the errors in E_{iso} and $E_{\mathrm{peak}}^{\mathrm{src}}$. Here, n is the number density of the ambient (uniform) medium, and η_γ is the efficiency of the shock in converting the energy in the ejecta into γ-rays. See §3.1 for more explanations.
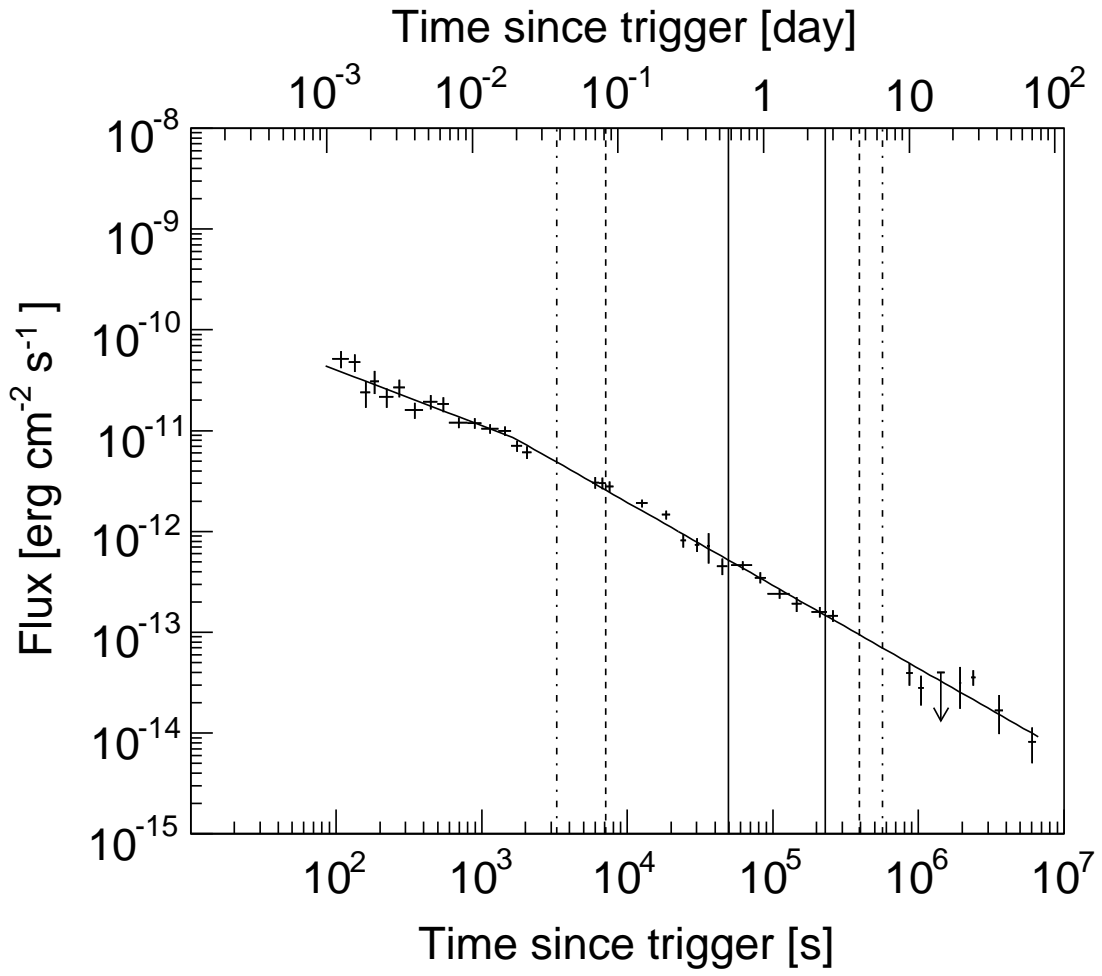
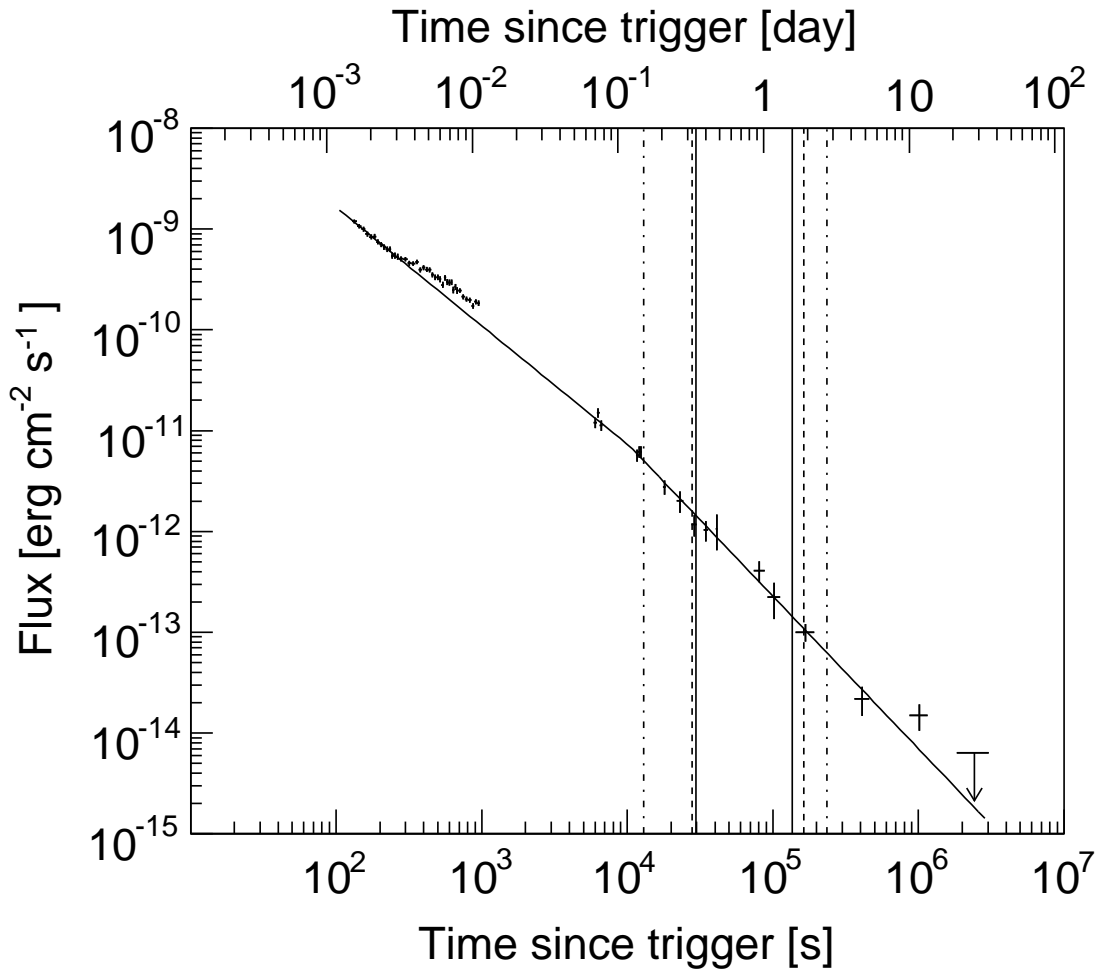Fig. 2.— The same as Fig. 1 but for XRF 050416a.
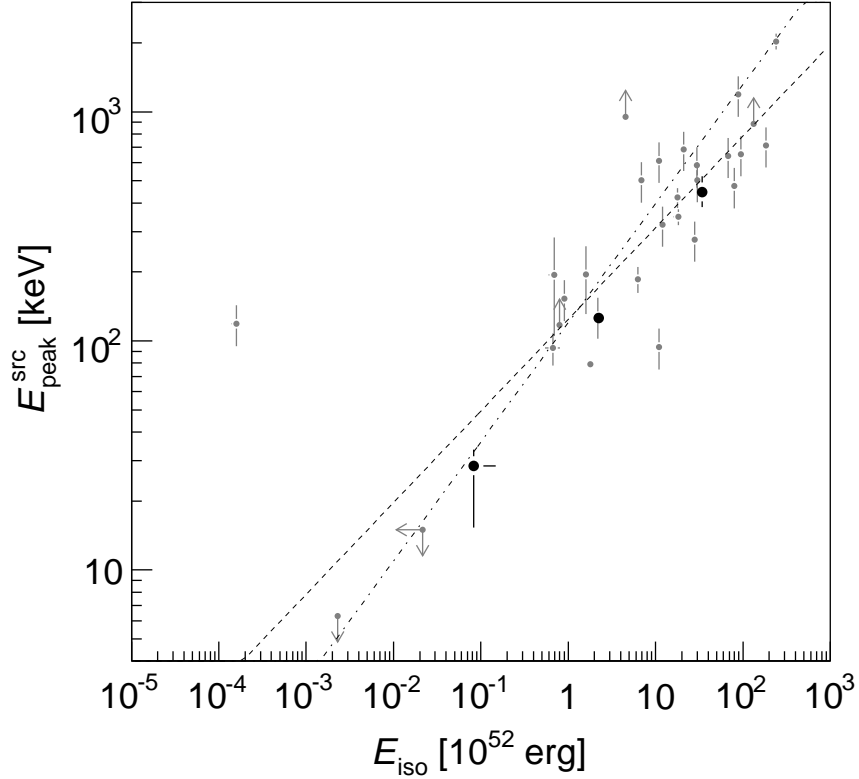
Fig. 3.— The same as Fig. 1 but for GRB 050525a.

Fig. 4.— Locations of GRBs in the $(E_{\rm iso}, E_{\rm peak}^{\rm src})$-plane, where $E_{\rm iso}$ is the isotropic-equivalent energy and $E_{\rm peak}^{\rm src}$ is the peak energy of the burst spectrum in the rest frame of the burst. The three filled black circles correspond (from lower left to upper right) to XRF 050416a, GRB 050525a, and GRB 050401. The burst locations previously reported by Ghirlanda et al. (2004b) are shown as filled gray circles. The dashed and dot-dashed lines are the correlations between $E_{\rm iso}$ and $E_{\rm peak}^{\rm src}$ reported by Amati et al. (2002) and Ghirlanda et al. (2004b), respectively. The locations of XRF 050416a, GRB 050525a, and GRB 050401, derived from Swift and Konus-Wind observations, lie within the scatter of the previous $E_{\rm iso}$–$E_{\rm peak}^{\rm src}$ relation.
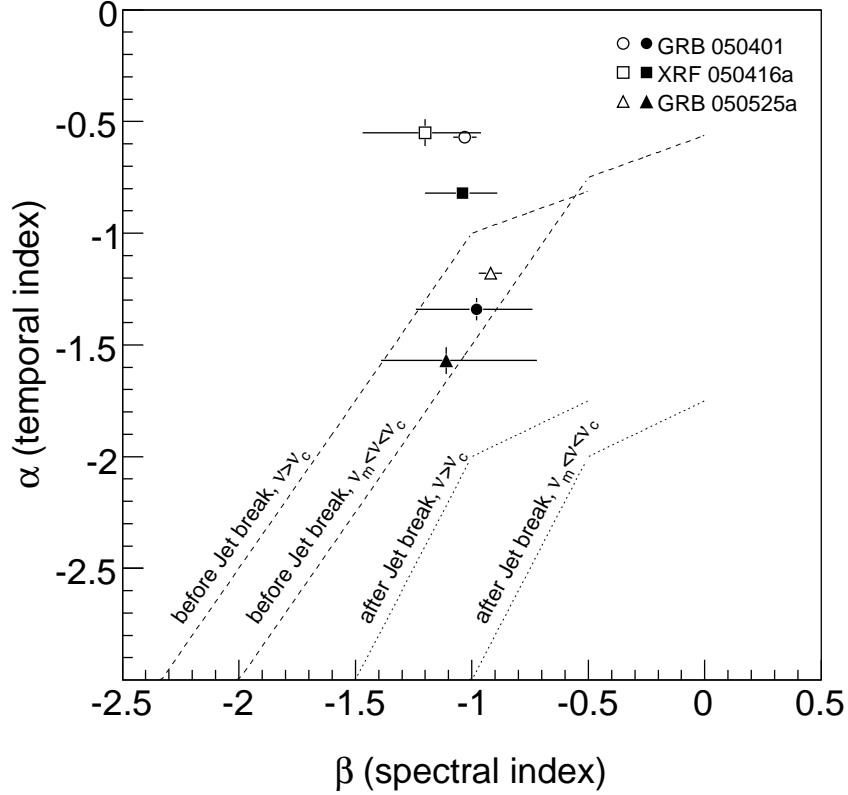
Fig. 5.— Expected relation between the temporal index α and the spectral index $\beta(= -\Gamma + 1)$, assuming a uniform density (corresponding to an ISM environment) and that the external shock has reached the slow-cooling phase. The open symbols show the locations of GRB 050401, XRF 050416a, and GRB 050525a, prior to the X-ray break at t_b, while the closed symbols shows the locations of the three bursts after the break. None of the three bursts satisfy the post-break relations expected in the standard afterglow model.
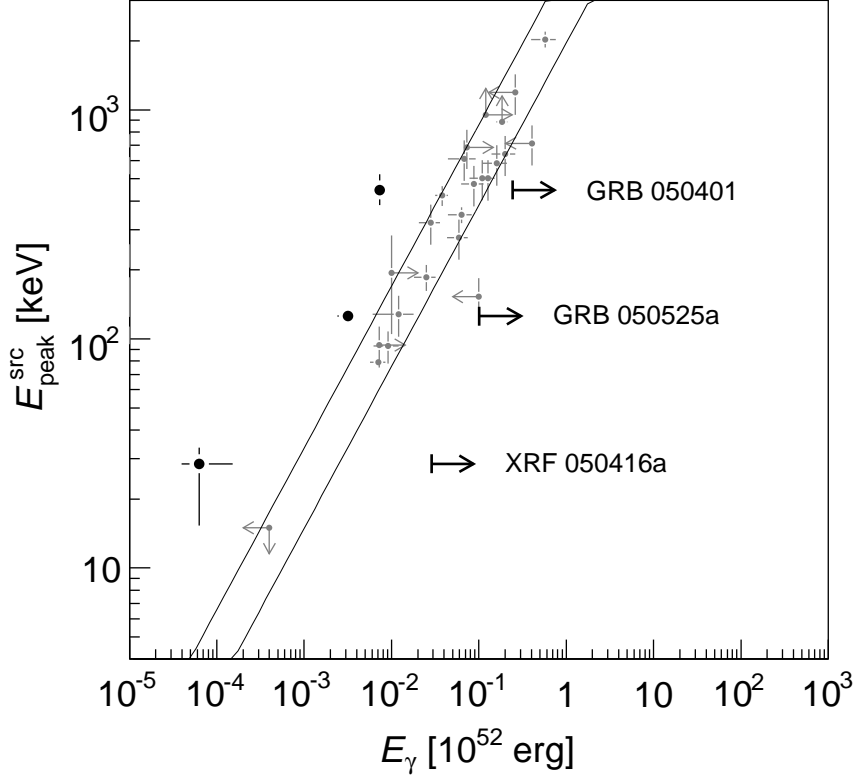
Fig. 6.— Locations of GRBs in the $(E_\gamma, E_{\text{peak}}^{\text{src}})$-plane, where E_γ is the collimation-corrected energy and $E_{\text{peak}}^{\text{src}}$ is the peak energy of the burst spectrum in the rest frame of the burst. The locations of the bursts in the samples of Ghirlanda et al. (2004b) are plotted as filled gray circles. All of the bursts with well-constrained values of E_γ and $E_{\text{peak}}^{\text{src}}$ in the Ghirlanda et al. (2004b) sample lie inside the two solid diagonal lines corresponding to the Ghirlanda relation (Eq. 1) calculated for $A = 1950$ keV and $A = 4380$ keV. In the cases of GRB 050401, XRF 050416a, and GRB 050525a, no jet break was observed in the X-ray afterglow light curve at an epoch which would allow E_γ and $E_{\text{peak}}^{\text{src}}$ to lie in the band between the two solid lines. The filled black circles show the locations of the three bursts, assuming that the X-ray break observed at an early time t_b is, in fact, the jet break. The lower limits on E_γ for the three bursts assume that the jet break occurs after the last Swift XRT observation of the X-ray afterglow. In either case, E_γ lies outside of the band defined by the two diagonal solid lines for all the three *Swift* bursts.